12-1-2010

The isotopic composition of Light-Enhanced Dark Respiration (LEDR) in C3 and C4 plants

Susan Mirabal

Susan Christy Mirabal

Candidate

Biology

Department

This thesis is approved, and it is acceptable in quality and form for publication:

Approved by the Thesis Committee:

,Chairperson

Todd Rosenstiel (proxy)

THE ISOTOPIC COMPOSITION OF LIGHT-ENHANCED DARK RESPIRATION (LEDR) IN C3 AND C4 PLANTS

BY

SUSAN CHRISTY MIRABAL

B.S. BIOLOGY

THESIS

Submitted in Partial Fulfillment of the
Requirements for the Degree of

Master of Science
Biology

The University of New Mexico
Albuquerque, New Mexico

December, 2010

DEDICATION

"'I want to ask you to do something,' said the wise man, handing the boy a teaspoon that held two drops of oil. 'As you wander around, carry this spoon with you without allowing the oil to spill.'

Upon returning to the wise man, he related in detail everything he had seen. 'But where are the drops of oil I entrusted to you?' asked the wise man. Looking down at the spoon, the boy saw that the oil was gone.

'Well, there is only one piece of advice I can give you,' said the wisest of wise men.

'*The secret to happiness is to see all the marvels of the world, and never to forget the drops of oil on the spoon*.'"

– The Alchemist, Paulo Coelho

To Norma Edith Monzón de Sánchez

ACKNOWLEDGEMENTS

Thanks to Dr. Margaret Barbour for valuable discussion on the project. To my committee members Dr. William Pockman and Dr. Todd Rosenstiel for their patience and understanding. To Joy Avritt, Daniella E. McCade, Dianne Pater and Lindsey Boren for help with the research plants. And to Harper Baird for her editorial insight.

Special thanks to my committee chair, Dr. David Hanson for his mentoring, guidance and support throughout my professional career.

Financial support for this project was provided by NSF grant 0719118 and the Grove Summer Scholarship from the Department of Biology, UNM. Funding for the presentation of this research at the American Society of Plant Biologist (ASPB) 2009 and 2010 meetings was provided by the UNM Research and Professional Travel Award from the Office of Graduate Studies, the UNM the Student Conference Award Program from the Office of Career Services, the Bealmer Scholarship from the UNM Department of Biology, and a travel award from ASPB.

THE ISOTOPIC COMPOSITION OF LIGHT-ENHANCED DARK RESPIRATION (LEDR) IN C3 AND C4 PLANTS

BY

SUSAN CHRISTY MIRABAL

ABSTRACT OF THESIS

Submitted in Partial Fulfillment of the
Requirements for the Degree of

Master of Science
Biology

The University of New Mexico
Albuquerque, New Mexico

December, 2010

The Isotopic Composition of Light-Enhanced Dark Respiration (LEDR)

in C_3 and C_4 plants

by

Susan Christy Mirabal

B.S., Biology, University of New Mexico, 2008

M.S., Biology, University of New Mexico, 2010

ABSTRACT

Light-enhanced dark respiration (LEDR) has been studied in C_3 plants as a method to elucidate the careful balance between photosynthesis and respiration yet little is known about the metabolic properties by which it occurs in C_4 plants.

Using a tunable diode laser gas exchange system, we analyzed transient isotopic shifts in leaf-respired CO_2 associated with LEDR at 10Hz frequency from *Populus deltoides* (C_3), *Amaranthus hypochondriacus* (C_4 NAD-ME), and *Zea mays* (C_4 NADP-ME). The results suggest that:

(1) Post-photosynthetic fractionations are different between C_3 and C_4 (and within C_4) plants, where *A. hypochondriacus* exhibited an unexpected LEDR response (Fig. 3, Table 3),

(2) In *Z. mays*, post-illumination respiration was not dependent on light but its isotopic composition ($\delta^{13}C_{RL}$) reflected changes in the previous illumination period. Depleted values of $\delta^{13}C_{RL}$ found here may be due to NADP-malic enzyme fractionation, and

(3) The decarboxylation of various metabolic substrates is likely responsible for the differing post-illumination respiration responses in all species. Especially important are malate decarboxylation (in *P. deltoides*) and pyruvate decarboxylation (in *A. hypochondriacus* and *Z. mays*).

We attributed the differences in the isotopic composition of LEDR in the above-mentioned plant species to variations in their cellular metabolism, compartmental fractionation and mesophyll and bundle sheath leakiness.

TABLE OF CONTENTS

INTRODUCTION

Light-enhanced dark respiration (LEDR) is an increase in CO_2 evolution following a period of illumination reflecting an increased supply of non-respiratory substrates (Atkin *et al.* 2000, Atkin *et al.* 1998). LEDR increases with increasing light in the preceding light period and is therefore a function of the photosynthetic CO_2 fixation rate in that period (Azcon-Bieto and Osmond 1983, Reddy *et al.* 1991, Hill and Bryce 1992, Xue *et al*. 1996, Igamberdiev 1997, Atkin *et al*. 1998). In C_3 plants, LEDR has been studied as a method to elucidate the careful balance between photosynthesis and respiration (Tcherkez and Farquhar 2005). Maintaining balance is crucial for adequate plant function as respiration is more complex than photosynthesis, requiring many metabolic and biochemical pathways used to generate energy in the form of ATP and NAD(P)H (Cannell and Thornely 2000).

Many properties regarding LEDR in C_3 plants have been discovered in the past decade including its dependence on the concentration of O_2 and CO_2 (Atkin *et al.* 1998, Atkin *et al.* 2000); its enrichment in ^{13}C (Barbour *et al.* 2007), which correlates with malate accumulation in the light and rapid malate decarboxylation after the onset of darkness (Tcherkez and Farquar 2005, Gessler *et al.* 2009); the involvement of the enzyme phospho*enol*pyruvate carboxylase (PEPc) in CO_2 enrichment (Barbour *et al*. 2007). The factor(s) responsible for LEDR are closely related to the factor(s) that govern light inhibition of respiration suggesting an involvement of photosynthetic enzymes in the regulation of respiration (Atkins *et al.* 1998).

Much uncertainty still surrounds the mechanistic process by which post-illumination respiratory responses, such as LEDR, occur in C_4 plants as these have a

more complex cell structure and metabolism (Parys and Jastrzebski 2006). C_4 plants spatially separate the two main CO_2-fixing enzymes, PEPc, and ribulose 1, 5-bisphosphate carboxylase oxygenase (Rubisco), into the mesophyll and bundle sheath cells respectively (Bjorkman and Gauhl 1969, Hatch and Slack 1970, Hatch 1999). This structural arrangement gives rise to the biochemical properties that allow C_4 plants higher photosynthetic rates by increasing the concentration of CO_2 around the active site of Rubisco (Hatch and Slack 1969). This adaptation evolved independently more than 45 times in over 19 families of angiosperms, and thus represents one of the most convergent of evolutionary phenomena (Sage 2004). There are three metabolic subgroups for CO_2 fixation in the C_4 pathway: NAD-ME (Hatch and Kagawa 1974) (Fig. 1), NADP-ME (Hatch and Slack 1970) (Fig. 2) and PEP-CK (Edwards *et al.* 1971). These C_4 variations represent a mixture of photosynthetic and metabolic mechanisms giving rise to different properties depending on the plant species and environment (Farquhar *et al.* 1989).

LEDR has been recorded in protoplasts of various C_4 types where lower rates of photosynthesis in the light lowered the magnitude of LEDR (Parys and Jastrzebski 2006). But studies of the effect of light on respiration *in vivo* or whole C_4 leaves have not been undertaken to date.

Many characteristics of the LEDR response in C_4 plants are still unknown such as the extent of ^{13}C enrichment and the role of photosynthetic enzymes and pathways in regulating respiration. It is well known that PEPc activity is greater in C_4 plants and has a much larger effect on the isotopic signature than in C_3 plants (Farquhar *et al.* 1989). And that photosynthetic discrimination is not significantly different between NAD-ME and NADP-ME C_4 types at high light although differences in leaf carbon isotope composition

has been observed between the two subgroups (Cousins *et al.* 2008). The effects of post-photosynthetic fractionation on CO_2 isotopologues including the effects of subsequent metabolism of photosynthetic products such as when metabolites are inter-converted or when they are decarboxylated (Gessler *et al.* 2009) is still being investigated.

Current models do not account for differences in post-photosynthetic fractionation between C_3 and C_4 plants or within C_4, and in general, these fractionations are thought to be minor (Evans *et al.* 1986). Though recent work suggests they may be significant in C_3 plants (Tcherkez *et al.* 2008). Isotopic models also do not account for transient changes in the isotopic composition that can be caused by metabolic imbalances induced by rapidly changing environmental conditions. While these transients are unlikely to have a large impact on the isotopic composition of a leaf, they do provide unique insight into *in vivo* metabolism, potentially including enzyme activities, and explain why short-term measurements of isotopic gas exchange can greatly deviate from the long-term tissue composition.

Here, we examined the LEDR response as well as its isotopic signature ($\delta^{13}C_{RL}$) in *Populus deltoides* (C_3), *Amaranthus hypochondriacus* (NAD-ME C_4) (Murmu *et al.* 2003) and *Zea mays* (NADP-ME C_4) to determine the differences in discrimination against $^{13}CO_2$ as well as the potential source of LEDR in C_4 plants using a $^{13}CO_2$ label.

MATERIALS AND METHODS

Plant material and growth conditions

Poplar (*P. deltoides)*, amaranth (A. hypochondriacus*)* and corn (*Z. mays)* seeds were

grown in Metro-Mix 360 media (Scotts, Marysville, OH, USA) under atmospheric conditions in a growth chamber at the University of New Mexico in Albuquerque, NM. All plants were exposed to 12-hour days (25°C/22°C day/night) at 1000 μmol photons m^{-2} s^{-1}, transferred to 3.8L pots one week after germination, and fertilized with Ironate (Hi-Yield, Bonham, TX, USA) and MultiCote all-purpose plant food 18-6-12 (N: P: K) (Schultz, St. Louis, MO, USA) when needed. The plants were watered every other day and sampled 5 weeks after germination.

Leaf gas exchange and isotopic measurements

The 5^{th} or 6^{th} leaf was exposed to three photosynthetically active radiation (PAR) levels: 1170 (± 2.4), 350 (± 3.5) and 130 (± 2.1) μmol photons m^{-2} s^{-1} until a steady state was reached, then dark adapted for the subsequent 30 minutes. Light intensities were manually adjusted using an external 20cm x 20cm white LED light source (SL 3500, Photo Systems Instruments, Drasov, Czech Republic) and confirmed with a quantum sensor (LI-190, Li-Cor, Inc., Lincoln, NE, USA).

Net CO_2 exchange and stomatal conductance were measured using a portable photosynthetic system (LI6400, Li-Cor, Inc., Lincoln, NE, USA) fitted with a custom-built large leaf chamber (similar to Barbour *et al.* 2007) coupled to a tunable diode laser (TDL) absorption spectrometer (TGA100A, Campbell Scientific, Inc., Logan, UT, USA) to measure the real-time isotopic discrimination against $^{13}CO_2$ at 10Hz frequency. All data were corrected for actual leaf areas ranging from 22.4cm^2 to 57.3cm^2. Leaf temperature averaged 25.6ºC (± 0.27) for all plants. For the LEDR measurements, the LI6400 system was used to maintain the CO_2 concentration at 400μmol mol^{-1} (in both the

light and dark) flowing at 600μmol s^{-1} in the light and 300μmol s^{-1} in the dark. CO_2 going into the chamber was scrubbed with desiccant to remove water.

^{13}C Labeling experiments

Immediately after the LEDR measurements, leaves of the above-mentioned plants were allowed to reach a steady state at 1170 (± 2.9) μmol photons m^{-2} s^{-1} with an atmospheric $^{13}CO_2$ source of -4‰, then exposed to a heavy labeled source of +148‰ $^{13}CO_2$ for 2, 5 or 10min. The leaves were subsequently switched to the -4‰ $^{13}CO_2$ source and dark adapted for 30min. One -4 and one +148‰ $^{13}CO_2$ tank were used for all of the measurements.

A +148‰ $^{13}CO_2$ tank was made by acidifying 99% $H^{13}CO_2$ (Cambridge Isotope Laboratories, Andover, MA, USA) and volatilizing it in an extraction line. The resulting CO_2 was transferred to an evacuated cylinder and -4‰ $^{13}CO_2$ was added to generate the desired isotopic composition (+148‰ $^{13}CO_2$). A custom system of mass flow controllers (MKS instruments, Andover, MA, USA) connected to a digital multi-gas controller (Model 647C, MKS instruments, Andover, MA, USA) was used to combine N_2, O_2 and +148‰ $^{13}CO_2$ from gas cylinders to the desired composition. The total flow rate was split and delivered directly to the LI6400 leaf chamber and reference infra-red gas analyzer (IRGA) with additional mass flow controllers such that the flow to the leaf matched the LI6400 flow rate with excess directed to the reference. Switching between the LI6400 controlled gas mixture with -4‰ $^{13}CO_2$ and the custom mass flow controller system with +148‰ $^{13}CO_2$ was accomplished using manually operated 3-way valves located between the LI6400 console and leaf chamber. Switching in this manner changed the composition of gas above the leaf within 1min (data not shown).

Discrimination and isotopic composition calculations

Net $^{13}CO_2$ discrimination in the light (Δ), described as per mil (‰), was calculated following Evans *et al.* (1986):

$$\Delta = \frac{\xi\,(\delta^{13}C_o - \delta^{13}C_e)}{1000 + \delta^{13}C_o - \xi\,(\delta^{13}C_o - \delta^{13}C_e)}, \quad (1)$$

where

$$\xi = C_e / (C_e - C_o), \quad (2)$$

and C_e is the concentration of CO_2 entering the leaf chamber with $\delta^{13}C_e$ representing the isotopic composition associated with C_e. C_o is the concentration of CO_2 exiting the leaf chamber and $\delta^{13}C_o$ is its corresponding isotopic signature.

Leaf-respired isotopic composition ($\delta^{13}C_{RL}$) is reported here relative to the Pee Dee Belemnite (PDB) standard (Evans *et al.* 1986, Barbour *et al*. 2007):

$$\delta^{13}C_{RL} = \frac{\delta^{13}C_o - \delta^{13}C_e\,(1 - p)}{p}, \quad (3)$$

where,

$$p = (C_o - C_e) / C_o. \quad (4)$$

Enzymatic assay

PEPc activity was determined from fresh leaf punches exposed to 1170 μmol photons m^{-2} s^{-1} as described by Duff and Chollet (1995) and Rosenstiel *et al.* (2004) with the

following modifications: 50mg of plant material was ground in 100mM Tricine-KOH (pH 8.0) buffer containing 5mM $MgCl_2$, 5% (v/v) glycerol, 0.25mM EDTA, 14mM β-mercaptoethanol, 1mM PMSF and 2% (w/v) PVP-40. The resulting mixture was centrifuged at 14,000rpm for 15sec at -4°C and 20µL of supernatant was immediately assayed using the spectrophotometric methods at A_{340} outlined in Rosenstiel *et al.* (2004).

Statistical analyses

All statistical analyses were performed using Sigma Plot (Systat Software Inc., San Diego, CA, USA). A one-way analysis of variance (ANOVA) was used to assess the differences in PEPc activity between plant types and in net CO_2 exchange and $\delta^{13}C_{RL}$ when appropriate. Significant results when assumed when $p < 0.05$.

RESULTS

To further understand the differences in LEDR in C_3 and C_4 plant species, I exposed leaves of poplar, amaranth and corn to different light intensities prior to the dark, quantified PEPc activity, and labeled the last 2, 5 or 10min of illumination with CO_2 enriched in ^{13}C before a dark period. For clarity, only one representative replicate of the light and labeling experiments are plotted on Figures 3 and 5, the average and standard deviation for the replicates are presented on Tables 1-3.

The magnitude and isotopic composition of LEDR

The magnitude of the LEDR response and its corresponding $\delta^{13}C_{RL}$ varied with each plant species (Fig. 3). *P. deltoides* showed a classic LEDR as observed in other C_3

species such as *Nicotiana tabaccum* where the magnitude of post-illumination respiration increased with increasing light (Fig. 3). LEDR also showed increasing enrichment with exposure to light (Fig. 3, Table 1).

A small LEDR response was recorded from A. hypochondriacus displaying an enriched $\delta^{13}C_{RL}$ and higher steady state photosynthetic values than *Z. mays* at 1170 PAR (Fig. 3, Table 1). Smaller post-illumination respiratory responses were recorded at 350 and 130 PAR showing little or reversed $\delta^{13}C_{RL}$ response respectively (Fig. 3, Table 1). The $\delta^{13}C_{RL}$ steady state values became more enriched with decreasing light (Table 1).

The post-illumination respiration response in *Z. mays* was not consistently enhanced by light as it only changed between the lowest two light intensities (Fig. 3, Table 1). The isotopic signature was more variable showing either no relationship or the opposite relationship to that of the other species (Fig. 3, Table 1). Like in *A. hypochondriacus,* the $\delta^{13}C_{RL}$ steady state values became more enriched with decreasing light (Table 1). Values associated with the photosynthetic rates at 1170, 350 and 130 PAR for all sampled plants are listed in Table 2.

Figure 4 shows net CO_2 exchange and $\delta^{13}C_{RL}$ versus photosynthetic rate for all sampled plants at all light intensities. In *P. deltoides*, net CO_2 exchange and $\delta^{13}C_{RL}$ significantly increased with increasing photosynthetic rate during the preceding light period ($R^2 = 0.99$ and 0.96 respectively). *A. hypochondriacus* shows a similar trend in net CO_2 exchange ($R^2 = 0.99$) yet it is less significant between $\delta^{13}C_{RL}$ and photosynthetitc rate ($R^2 = 0.67$). *Z. mays* shows a significantly reversed isotopic response between $\delta^{13}C_{RL}$ and photosynthetic rate ($R^2 = 0.99$) (Fig. 4).

Labeling LEDR

To assess both the incorporation and the extent of LEDR labeling, a heavy isotope of $^{13}CO_2$ (+148 ‰) was applied for 2, 5 or 10min at 1170 PAR. In *P. deltoides*, this label resulted in a significant increase in enrichment of the isotopic signature of LEDR with increasing label time ($p = 0.001$, Fig. 5, Table 3). A small pulse release of label occurred 5min after the LEDR peak (Fig. 5). An enrichment in the $\delta^{13}C_{RL}$ steady state occurred from -28‰ when no label was applied, to a steady state of -24‰ for the 2 and 5min label, and to a steady state of -12‰ for the 10min label (Fig. 5, Tables 1, 3).

LEDR becomes significantly enriched with increasing label time in A. hypochondriacus (C_4 NAD-ME) ($p = 0.01$, Fig. 5, Table 3). The label was released steadily over 30min with little to no visible $\delta^{13}C_{RL}$ peak accompanying LEDR (Fig. 5, Table 3). The $\delta^{13}C_{RL}$ values at 25min increased from -16‰ at the steady state without label to +0.83‰ with the 2min label, -13‰ in the steady state without label to +7.87‰ with the 5min label and from -9‰ in the steady state without label to +65‰ with the 10min label (Tables 1, 3).

The 2min ^{13}C label resulted in a significant increase in the enrichment of CO_2 evolved at 1170 PAR in *Z. mays* ($p = 0.01$, Fig. 5, Table 3). The CO_2 becomes more enriched with labeling time; quickly releasing the $^{13}CO_2$ provided approximately 7min after switching to the dark, in a more distinct and delayed pulse than in *P. deltoides* or *A. hypochondriacus* (Fig. 5). Continued release of the $^{13}CO_2$ label in all species was observed after 30min (Table 3).

Stomatal conductance (g_s) for LEDR and labeling experiments in all plants varied little in the light to dark transitions (Fig. 6).

Enzymatic analysis

The activity of PEPc was determined in *P. deltoides*, A. hypochondriacus and *Z. mays* leaves exposed to 1170 PAR. A. hypochondriacus showed a significantly higher amount of PEPc activity (20.1 μmol mg chlorophyll^{-1} min^{-1}) than *Z. mays* (15.3 μmol mg chlorophyll^{-1} min^{-1}) and *P. deltoides* (1.1 μmol mg chlorophyll^{-1} min^{-1}), ($p<0.001$) (Fig. 7).

DISCUSSION

Respiration immediately following illumination has been examined for plants utilizing three photosynthetic pathways (Fig. 3). While the main sources of CO_2 evolution for each species are discussed below, it should be noted that the dynamic response of respiration we observed in the first few minutes of darkness is not likely to be due to the diffusion of HCO_3 out of the cell. The activity of carbonic anhydrase facilitating the release of HCO_3 accumulated in the stroma during the illumination occurs too quickly (within 100sec after dark) to account for the peak post-illumination respiration (Badger *et al.* 1993, Hanson *et al.* 2002). Instead, the amount and timing of CO_2 released is at least partly due to malate decarboxylation (Gessler *et al.* 2009), and may also indicate the ease of CO_2 exchange between the chloroplast and the atmosphere.

Another potential source of the CO_2 released during post-illumination respiration may be due to pyruvate decarboylation. In the absence of oxygen, the decarboxylation of pyruvate to acetaldehyde by pyruvate decarboxylase has been recorded in leaves incubated with nitrogen (Kimmerer 1987, Kimmerer and MacDonald 1987).

Acetaldehyde synthesized by pyruvate metabolism in the previous light period is released approximately 2-3 minutes after dark adaptation (Karl *et al*. 2002).

Photosynthetic-dependency of LEDR and $\delta^{13}C_{RL}$ in C_3 plants

LEDR reflects the amount of photosynthetic metabolites available to the mitochondria following a period of illumination (Hill and Bryce 1992, Xue *et al.* 1996, Igamberdiev *et al.* 1997, Atkin *et al.* 1998, Padmasree and Raghavendra 1999). The LEDR in *P. deltoides* shown here (Fig. 3, Table 1) supports previous LEDR experiments in C_3 species such as castor bean, bean, tobacco and sunflower, (Barbour *et al.* 2007, Ghashghaie *et al.* 2001, Atkin *et al.*1998, Xu *et al.* 2004) where the photosynthetic rate in the previous light period is in part determined by the amount of light provided (Table 1), (Atkin *et al.* 1998). In *P. deltoides*, periods of high post-illumination respiration released CO_2 enriched in ^{13}C as seen by Barbour *et al.* (2007). The steady state $\delta^{13}C_{RL}$ values for *P. deltoides* (-30‰, Fig. 3) presented here are also similar to those published by Xu *et al.* (2004) of approximately -26‰.

The metabolic origin of LEDR in C_3 plants needs further clarification. Among the hypotheses, the decarboxylation of malate as the source of CO_2 for LEDR (Farqhuar *et al.* 1989, Atkin *et al.* 1998, Raghavendra *et al.* 1994, Xu *et al.* 1996, Barbour *et al.* 2007, Gessler *et al.* 2009, Werner *et al.* 2009) has been investigated recently. We applied a short-term (2min or less) $^{13}CO_2$ label in the previous light period to label pools of recently-fixed substrates and compare this response to those observed with longer label times (Basssham *et al.* 1950). The labeling experiments presented here suggest the involvement of malate decarboxylation in supplying the CO_2 evolved as the LEDR peak

is labeled after a rapid 2min supply of $^{13}CO_2$ (Fig. 5, Fig. 8, Table 3). It has been shown that the decarboxylation malate occurs within the first few minutes after dark adaptation in barley mesophyll protopasts (Hill and Bryce 1992) and that 22% of the CO_2 released during LEDR is due to the decarboxylation of malate in *Ricinus communis* (Gessler *et al.* 2009). A rapid release of the label during LEDR suggests that recently synthesized malate is potentially released sooner than stored non-labeled malate pools, as the latter would cause ^{13}C depletion rather than the observed enrichment during LEDR (Fig. 5, Fig. 8, Table 3). LEDR also became more enriched the longer the $^{13}CO_2$ label was applied at high light (Fig. 5, Table 3) suggesting perhaps that more malate is being labeled and subsequently decarboxylated in the dark.

The involvement of other decarboxylases or substrates in the release of CO_2 during LEDR is not likely as the predicted isotopic shifts potentially caused by the TCA cycle and key enzymes (such as pyruvate dehydrogenase and citrate synthase, both critical in the conversion of pyruvate to acetyl-CoA and acetyl-CoA to citrate respectively) have failed to provide the observed dynamics in respiratory $\delta^{13}C$ (Werner *et al.* 2009). The transient release of acetaldehyde during LEDR has been suggested by Karl *et al*. (2002), and is potentially due to the buildup of cytosolic pyrvuvate when key enzymes are inhibited in the dark and when pyruvate transport into the mitochondria decreases (2002). This transient release is due to the equilibration of pyruvate concentrations after release in the dark, decreasing the potential pool of pyruvate for decarboxylation by pyruvate decarboxylase and thereby decreasing acetaldehyde formation (Karl *et al.* 2002). The direct involvement of pyruvate decarboxylase in LEDR has not been tested in these experiments and, because of the non-specific ^{13}C label

applied, we cannot exclude the decarboxylation of other compounds as contributing sources of evolved CO_2.

While non-carboxylation isotope effects such as a diffusional gas barrier against evolved CO_2 could also play a part in the steady release of label after LEDR, it is likely that an enriched pool of non-malate substrates (or other Rayleigh fractionation processes of ^{13}C – discriminating enzymes) is responsible for the transient post-LEDR changes in $\delta^{13}C_{RL}$ (Werner *et al.* 2009). Hence the steady release of the non-specific $^{13}CO_2$ label after LEDR is likely due to the continued released of other labeled compounds or pools (Fig. 5).

Potential LEDR sources in NAD-ME and NADP-ME C_4 plants

The complex metabolic interactions in C_4 plants that allow higher photosynthetic capacity also make the determination of LEDR properties more difficult (Parys and Jastrzebski 2006). *A. hypochondriacus* uses the NAD-ME pathway (Fig. 1) which like the NADP-ME pathway (Fig. 2), spatially separates the two main CO_2-fixing enzymes, PEPc and Rubisco, allowing an increased concentration of CO_2 near the active site of Rubisco thereby increasing its photosynthetic capacity (Kanai and Edwards 1999, Sage 2004).

A. hypochondriacus displayed increased photosynthetic rates yielding an LEDR response (Fig. 3) previously recorded only in C_3 plants (Atkin *et al.* 1998) contradicting observations made by Parys and Jastrzebski (2006) in *Panicum miliaceum* protoplasts. In addition, the isotopic composition of LEDR from *A. hypochondriacus* was less enriched when light intensity decreased, opposite to C_3 plants (Fig. 3, Fig. 4). The leaf material of NAD-ME species is also depleted in ^{13}C compared to NADP-ME C_4 type however, this

depletion is not reflected in photosynthetic discrimination (Cousins *et al*. 2008). Until now, enhanced post-illumination respiration did not vary with light intensity. Enhanced post-illumination respiration was believed to reflect only the amount of metabolites accumulated during the light (such as malate) and mitochondrial frequency (Parys and Jastrzebski 2006). But the increased photosynthetic capacity and alternate pathways in C_4 plants may lead to the accumulation of additional substrates that are subsequently released in the dark.

The $^{13}CO_2$ label was released steadily over 30min without a clear pulse release normally associated with LEDR after 5min of labeling with $^{13}CO_2$ (Fig. 5). The rapid enrichment of LEDR (after a 2min addition of $^{13}CO_2$) suggests the involvement of malate as a likely initial source of evolved CO_2 (Fig. 1). Increased labeling time further enriched the isotopic signature of LEDR (Fig. 5) also suggesting that, despite the metabolic differences between the C_3 and the C_4 NAD-ME pathway, the other respiratory substrates are also decarboxylated in the subsequent dark period (Parys and Jastrzebski 2006). The rate of oxidation of malate in the mesophyll and bundle sheath mitochondria from some C_4 plants is also higher than that of other substrates in the TCA cycle (Gardestrom and Edwards 1983, Ohnishi and Kanai 1983, Petit and Cantrel 1986, Parys and Jastrzebski 2006) suggesting that malate is the main CO_2 source in LEDR (Parys and Jastrzebski 2006) (Fig. 8). Mitochondrial frequency and the specific activity of mitochondrial enzymes is also higher in NAD-ME than NADP-ME C_4 types (Hatch and Carnal 1992) allowing faster malate decarboxylation in the subsequent dark period (Fig. 1). NAD malic enzyme activity is specific to the mitochondrial bundle shealth cells in *A. hypochondriacus* (Gutierrez *et al.* 1974, Long *et al.* 1994, Berry *et al.* 1997) localizing

and potentially delaying the release of CO_2 from conversion of malate to pyruvate in the bundle sheath cells.

The steady release of $^{13}CO_2$ after LEDR (Fig. 5, Table 3) is potentially due to the decarboxylation of pyruvate via the TCA cycle in the dark as the involvement of other molecules would shift the isotopic signature abruptly (Fig. 5, Fig. 8, Table 3). The release of CO_2 from labeled compounds in the TCA cycle for example, would result in a depletion of $^{13}CO_2$ (Gessler *et al.* 2009). Moreover, the steady decrease of pyruvate concentration immediately after dark has been recorded in other C_4 species such as *Z. mays* (Roeske and Chollet 1989). This slower release of label is different than that observed in C_3 *P. deltoides* where pyruvate may not play a part (Gessler *et al.* 2009).

The release of enriched CO_2 after labeling may also be due to increased leakiness of $^{13}CO_2$ out of the bundle sheath (Fig. 1, Fig. 8). Although leakage is suppressed by Kranz anatomy, a steep gradient of CO_2 concentration created between the mesophyll and bundle sheath cells in order to concentrate CO_2 around the active site of Rubisco (Farquhar 1983) leads to the greatest leakage recorded in NAD-ME C_4 plant types (Hattersley 1982) with 20% of CO_2 diffusing back into the mesophyll cells (Farquhar 1983, Lambers *et al.* 2008). Leakiness of CO_2 from the bundle sheath cells to the mesophyll may occur through the bundle sheath cell walls and may be facilitated by symplastic connections between the mesophyll and bundle sheath cells required for metabolite exchanges (Kromdijk *et al.* 2008).

The more complex model of C_4 photosynthetic carbon fixation, NADP-ME (Farquhar 1983) represented by *Z. mays*, displays an elevated rate of respiration shortly

after darkening a leaf that is unaffected by the previous light intensity as described by Parys and Jastrzebski (2006), (Fig. 3). The timing of this higher period of respiration is similar to that of LEDR in other species, however, the isotopic signature of respired CO_2 associated with the high respiration is inversely affected by PAR (Fig. 3). The $\delta^{13}C_{RL}$ is depleted with all light intensities suggesting that the source of CO_2 is different from that in plants with an LEDR response (Fig. 3, Fig. 2). Malic enzyme (ME) is responsible for the decarboxylation of malate and is found in NADP-ME plant types (Parys and Jastrzebski 2006) (Fig. 2). If the enzyme found in *Z. mays* is similar to the NADP-dependent malic enzyme from chicken liver that discriminates by 31‰ against ^{13}C (Edens *et al.* 1997, Hermes *et al.* 1982), then the decarboxylation of malate is likely the main source of evolved CO_2 during the high period of respiration. However, we have not tested this hypothesis and uncertainty still remains about other fractionations besides that produced by malic enzyme (Gessler *et al.* 2009).

CO_2 respired during this high rate post-illumination period becomes more enriched with labeling time, but also quickly releases the $^{13}CO_2$ provided in a more distinct and highly enriched and delayed pulse than that observed in either C_3 or C_4 NAD-ME plant types (Fig. 5, Table 3). These two responses, a relatively depleted value during peak respiration and an enriched $^{13}CO_2$ evolution afterward, are due to two potential sources of enriched metabolites (Fig. 2, Fig. 8). The evolved CO_2 peak in *Z. mays* is likely a combination of the decarboxylation of malate and pyruvate in both the mesophyll and bundle sheath cells (Fig. 7) (Roeske and Chollet 1989). The delayed and highly enriched response (approx. 7min into dark adaptation) has not been recorded before and therefore its metabolic source is more speculative. However, compartmentalization and

leakiness likely play a part in this response. Reduced leakiness has been shown for the NADP-ME C_4 types such as *Z. mays* because of the presence of suberized lamella (Hatch and Osmond 1976, Farquhar 1983, Hattersley 1982) potentially slowing diffusion out of the bundle sheath cells (and out to the mesophyll cells) shortly after darkness. If the CO_2 pool is slightly enriched over the mesophyll pool, then the slower diffusion would cause the observed enrichment. In addition, our data suggest that the faster efflux from the mesophyll cells is also larger as it has an effect on the net bulk CO_2 exchange rate (respiration is higher at the start of the dark period (Fig. 3, Fig. 8, Table 3)). If true, and if PEPc activity in the mesophyll is not strongly affected by light intensity, then this would explain the cause of the high period of respiration in the dark that is not enhanced by light but is still dependent on malate originating from PEPc activity.

The decarboxylation of the labeled pyruvate pool is likely the source of the steady release of $^{13}CO_2$ after LEDR (Fig. 8) since a decreased pool has been observed in *Z. mays* over a similar time frame (Roeske and Chollet 1989).

CONCLUSION

Dynamic isotopic composition changes of respiratory substrates (and thus changes in metabolic fluxes) may lead to intensive short-term changes in $\delta^{13}C$ (Gessler *et al.* 2009) not easily explained by transient $^{13}CO_2$ measurements and not detected by integrative tissue ^{13}C measurements. The general conclusions regarding the differences in LEDR and $\delta^{13}C_{RL}$ between C_3 and C_4 (NAD-ME and NADP-ME) plant species suggest that:

(1) LEDR is enriched:

a. In *P. deltoides* and *A. hypochondriacus* which increases with increasing light,

b. In *Z. mays*, the period of high respiration immediately following darkness was enriched in ^{13}C to a similar extent as other species, but this was not dependent on light intensity prior to darkening.

(2) The decarboxylation of malate (C_3) and both malate and pyruvate (C_4) are potential sources of rapidly evolved CO_2 after darkening,

(3) NAD-ME *A. hypochondriacus* exhibits an LEDR response where malate decarboxylation is the likely source of evolved CO_2 due to increased mitochondrial frequency and higher rates of malate oxidation,

(4) High post-illumination rates of respiration were not affected by light in the NADP-ME C_4 *Z. mays* but leaf-respired $^{13}CO_2$ ($\delta^{13}C_{RL}$) showed a dependence on the previous illumination period, and

(5) It is likely that the compartmentalization of various steps in the carbon-fixation reactions in NAD-ME and NADP-ME C_4 species leads to further fractionation that needs further investigation.

Future studies would include enzymatic analyses of key enzymes such as PDH, ICDH and 2-OGDH to quantify both their activity in the dark, as well as any net discrimination against $^{13}CO_2$ in the leaf. Determination of ^{13}C isotopic composition of bulk sugar, starch and lipids would provide information regarding the incorporation of the ^{13}C label. Finally, repetition of this study with a PCK-type C_4 species would further elucidate the differences in the C_4 pathway and give insight into the balance between photosynthesis and respiration in these grasses.

REFERENCES

Atkin OK, Evans JR, Siebke K (1998) Relationship between the inhibition of leaf transpiration by light and enhancement of leaf dark respiration following light treatment. Australian Journal of Plant Physiology 25: 437-443

Atkin OK, Millar AH, Gardestrom P, Day DA (2000) Dark Respiration in Leaves. In: "Photosynthesis: Physiology and Metabolism. Advances in Photosynthesis." Leegood RT, Sharkey TD and von Caemmerer S (eds), pp. 451-579. Kluwer, London

Azcon-Bieto J, Osmond CB (1983) Relationship between photosynthesis and respiration – The effect of carbohydrate status on the rate of CO_2 production by respiration in darkened and illuminated wheat leaves. Plant Physiology 71 (3): 574-581

Badger MR, Pfanz H, Bubel B, Heber U, Lange OL (1993) Evidence for the functioning of photosynthetic CO_2-concentrating mechanisms in lichens containing green algal and cyanobacterial photobionts. Planta 191 (1): 57-70

Barbour MM, McDowell NG, Tcherckez G, Bickford CP, Hanson DT (2007) A new measurement technique reveals rapid post-illumination changes in the carbon isotope composition of leaf-respired CO_2. Plant Cell and Environment 30: 469-482

Bassham JA, Benson AA, Calvin M (1950) The path of carbon in photosynthesis. VIII The role of malic enzyme. The Journal of Biological Chemistry 185 (2): 781-787

Berry JO, McCormac DJ, Long JJ, Boinski J, Corey AC (1997) Photosynthetic gene

expression in Amaranth, an NAD-ME type C_4 dicot. Australian Journal of Plant Physiology 24: 423-428

Bjorkman O, Gauhl E (1969) Carboxydismutase activity in plants with and without beta-carboxylation photosynthesis. Planta 88: 197-203

Cannell MR, Thornley JM (2000) Modeling the components of plant respiration: Some guiding principles. Annuals of Botany 85 (1): 45-54

Cousins AB, Badger MR, von Caemmerer S (2008) C_4 photosynthetic isotope exchange in NAD-ME and NADP-ME-type grasses. Journal of Experimental Botany 59 (7): 1695-1703

Duff SM, Chollet R (1995) In vivo regulation of wheat-leaf phospho*enol*puruvate carboxylase by reversible phosphorylation. Plant Physiology 107: 775-782

Edens WA, Urbauer JL, Cleland WW (1997) Determination of the chemical mechanism of malic enzyme by isotope effects. Biochemistry 36 (5): 1141-1147

Edwards GE, Kanai R, Black CC (1971) Phospho*enol*pyruvate carboxylkinase in leaves of certain plants which fix CO_2 by C_4-Dicarboxylic acid cycle of photosynthesis. Biochemical and Biophysical Research Communications 45 (2): 278-285

Evans JR, Sharkey TD, Berry JA, Farquhar GD (1986) Carbon isotope discrimination measured concurrently with gas exchange to investigate CO_2 diffusion in leaves of higher plants. Australian Journal of Plant Physiology 13: 281-292

Farquhar GD (1983) On the nature of carbon isotope discrimination in C_4 species. Australian Journal of Plant Physiology 10: 205-226

Farquhar GD, Ehleringer JR, Hubick KT (1989) Carbon isotope discrimination and

photosynthesis. Annual Review of Plant Physiology and Plant Molecular Biology 40: 503-537

Gardestrom P, Edwards GE (1983) Isolation of mitochondria from leaf tissue of *Panicum miliaceum*, a NAD-malic enzyme type-C_4 plant. Plant Physiology 71 (1): 24-29

Gessler A, Tcherkez G, Karyanto O, Keitel C, Ferrio JP, Ghashghaie J, Kreuzwieser J, Farquhar GD (2009) On the metabolic origin of the carbon isotope composition of CO_2 evolved from darkened light-acclimated leaves in *Ricinus communis.* New Phytologist 181: 374-386

Ghashghaie J, Duranceau M, Badeck FW, Cornic G, Adeline MT, Deleens E (2001) $\delta^{13}C$ of CO_2 respired in the dark in relation to $\delta^{13}C$ of leaf metabolites: comparison between *Nicotiana sylvestris* and *Helianthus annuus* under drought. Plant Cell and Environment 24 (5): 505-515

Gutierrez M, Gracen VE, Edwards GE (1974) Biochemical and cytological relationships in C_4 plants. Planta 119: 279-300

Hanson DT, Andrews TJ, Badger MR (2002) Variability of the pyrenoid-based CO_2-concentrating mechanism in hornwors (Anthocerotophyta). Functional Plant Biology 29 (2): 407-416

Hatch MD (1999) C_4 photosynthesis: A historical overview. In: "C_4 Plant Biology." Sage R and Monson R (eds), pp 17-46. Academic Press, New York

Hatch MD, Carnal NM (1992) The role of mitochondria in C_4 photosynthesis. In: "Molecular, biochemical and physiological aspects of plant respiration." Lambers H and van der Plas LHW (eds), pp 135-148. SPB Academic Publishing, The Hague

Hatch MD, Kagawa (1974) Activity, location and role of NAD malic enzyme in leaves with C_4 pathway photosynthesis. Australian Journal of Plant Physiology 1: 357-369

Hatch MD, Osmond, CB (1976). Compartmentation and transport in C_4 photosynthesis. In Encyclopedia of Plant Physiology, New Series, Vol 3, C.R. Stocking and U. Heber, eds (New York: Springer-Verlag), pp 144-184

Hatch MD, Slack CR (1969) Photosynthesis by sugar-cane leaves – A new carboxylation reaction and pathway of sugar formation. Biochemistry 101: 103-111

Hatch MD, Slack CR (1970) Photosynthetic CO_2-fixation pathways. Annual review of Plant Physiology 21: 141-162

Hattersley PW (1982) $\delta^{13}C$ values of C_4 types in grasses. Australian Journal of Plant Physiology 9: 139-154

Hermes JD, Roeske CA, O'Leary MH, Cleland WW (1982) Use of multiple isotope effects to determine enzyme mechanisms and intrinsic isotope effects – malic enzyme and glucose-6-phosphate-dehydrogenase. Biochemistry 21: 5106-5114

Hill SA, Bryce JH (1992) Malate metabolism and light-enhanced dark respiration in barley mesophyll protoplasts. In "Molecular, Biochemical and Physiological Aspects of Plant Respiration". II. Lambers and LHW van der Plas (eds), pp. 221-230. SPB Academic Publishing, The Netherlands

Igamberdiev AU, Zhou GQ, Malmberg G, Gasdestrom P (1997) Respiration of barley protoplasts before and after illumination. Physiologia Plantarum 99: 15-22

Kanai R, Edwards GE (1999) The biochemistry of C_4 photosynthesis. In: "C_4 Plant Biology." Sage RF and Monson RK (eds), pp 49-52. Academic Press, London

Karl T, Curtis AJ, Rosenstiel TN, Monson RK, Fall R (2002). Transient release of acetaldehyde from tree leaves – products of a pyruvate overflow mechanism? Plant, Cell and Environment 25: 1121-1131

Kimmerer TW (1987) Alcohol dehydrogenase and pyruvate decarboxylase activity in leaves and roots of eastern cottonwood (*Populus deltoides* Bartr) and soybean (*Glycine max L*). Plant Physiology 84: 1210-1213

Kimmerer TW, MacDonald RC (1987) Acetaldehyde and ethanol biosynthesis in leaves of plants. Plant Physiology 84: 1204-1209

Kromdijk J, Schepers HE, Albanito F, Fitton N, Carroll F, Jones MB, Finnan J, Lanigan GJ, Griffiths H (2008) Bundle sheath leakiness and light limitation during C_4 leaf and canopy CO_2 uptake. Plant Physiology 148: 2144-2155

Lambers H, Chapin III FS, Pons TL (2008) Plant physiological ecology, 2nd edition. Springer. New York, New York

Long JJ, Wang J-L, Berry JO (1994) Cloning and analysis of the C_4 photosynthetic NAD-dependent malic enzyme of amaranth mitochondria. Journal of Biological Chemistry 269: 2827-2833

Murmu J, Chinthapalli B, Raghavendra AS (2003) Marked modulation by the phosphate of phospho*enol*pyruvate carboxylase in the leaves of *Amaranthus hypochondriacus*, a NAD-ME type C_4-plant: decrease in malate sensitivity but no change in the phosphorylation status. Journal of Experimental Botany 54 (393): 2661-2668

Ohnishi J, Kanai R (1983) Differentiation of photorespiratory activity between mesophyll and bundle sheath cells of C_4 plants: glycine oxidation by mitochondria. Plant and

Cell Physiology 24 (8): 1411-1420

Padmasree K, Raghavendra AS (1999) Response of photosynthetic carbon assimilation in mesophyll protoplasts to restriction on mitochondrial oxidative metabolism: Metabolites related to the redox status and sucrose biosynthesis. Photosynthesis Research 62 (3): 231-239

Parys E, Jastrzebski H (2006) Light-enhanced dark respiration in leaves, isolated cells and protoplasts of various types of C_4 plants. Journal of Plant Physiology 163: 638-647

Petit P, Cantrel C (1986) Mitochondria from *Zea mays* leaf tissues – differentiation of carbon assimilation and photorespiratory activity between mesophyll and bundle sheath cells. Physiologia Plantarum 67 (3): 442-446

Raghavendra AS, Padmasree K, Saradadevi K (1994) Interdependence of photosynthesis and respiration in plant cells: interactions between chloroplasts and mitochondria. Plant Science 97: 1-14

Reddy MM, Vani T, Raghavendra AS (1991) Light-enhanced dark respiration in mesophyll protoplasts from leaves of pea. Plant Physiology 96: 1368-1371

Roeske CA, Chollet R (1989) Role of metabolites in the reversible light activation of pyruvate, orthophosphate dikinase in *Zea mays* mesophyll cells *in vivo*. Plant Physiology 90: 330-337

Rosenstiel TN, Ebbets AL, Khatri WC, Fall R, Monson RK (2004) Induction of poplar leaf nitrate reductase: A test of extrachloroplastic control of isoprene emission rate. Plant Biology (6): 12-21

Sage RF (2004) The evolution of C_4 photosynthesis. New Phytologist. 161: 341-370

Tcherkez G, Farquhar GD (2005) Carbon isotope effect predictions for enzymes involved in the primary carbon metabolism of plant leaves. Functional Plant Biology 32: 277-291

Tcherkez G, Bligny R, Gout E, Mahe A, Hodges M, Cornic G (2008) Respiratory metabolism of illuminated leaves depends on CO_2 and O_2 conditions. PNAS 105(2): 707-802

Werner C, Wegener F, Unger S, Nogues S, Priault P (2009) Short-term dynamics of isotopic composition of leaf-respired CO_2 upon darkening: measurements and implications. Rapid communications in mass spectrometry 23: 2428-1238

Xu C, Lin G, Griffin K, Sambrotto RN (2004) Leaf respiratory CO_2 is ^{13}C-enriched relative to leaf organic components in five species of C_3 plants. New Phytologist 163: 499-505

Xue XP, Gauthier DA, Turpin DH, Weger HG (1996) Interactions between photosynthesis and respiration in green algae *Chlamydomonas reinhardtii*: characterization of light-enhanced dark respiration. Plant Physiology 112: 1005-1014.

Figure 1. The C_4 NAD-ME Pathway, adapted from Kanai *et al.* 1999.

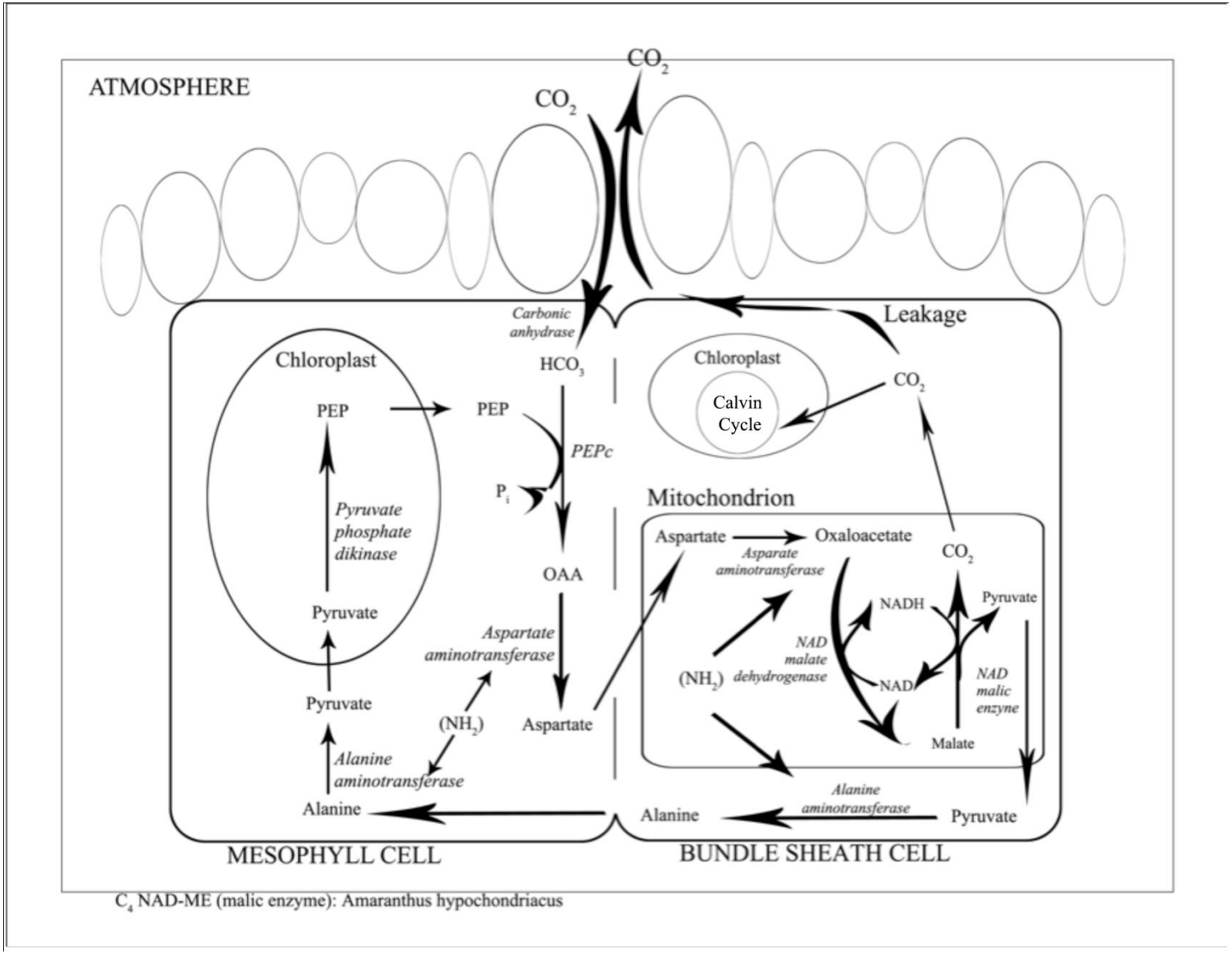

Figure 2. The C_4 NADP-ME pathway, adapted from Kanai *et al.* 1999.

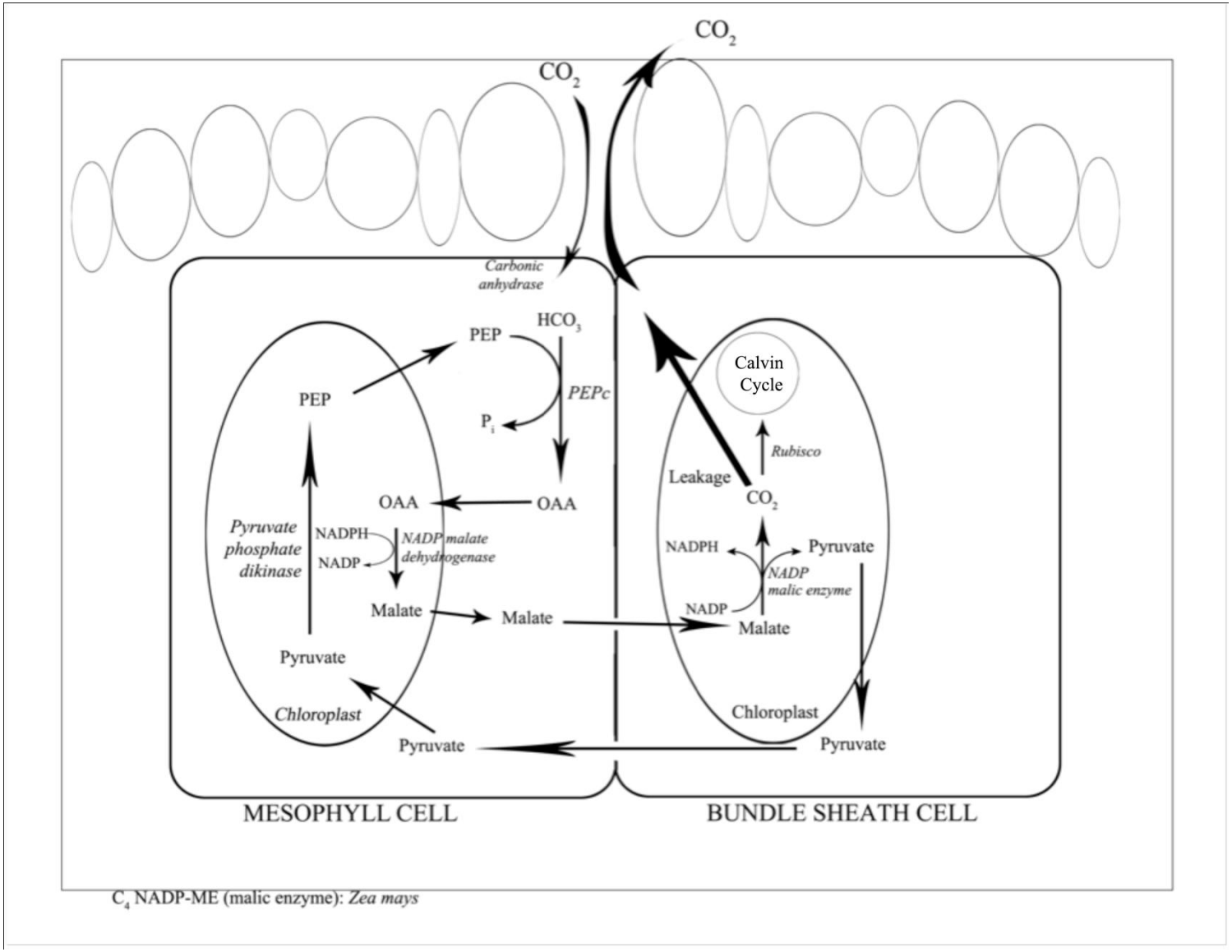

Figure 3. Light-Enhanced Dark Respiration (LEDR). Net CO_2 exchange (circles) and corresponding $\delta^{13}C_{RL}$ (triangles) for *P. deltoides* (**A**), *A. hypochondriacus* (**B**) and *Z. mays* (**C**) at 1170 (black), 350 (gray) and 130 (white) PAR for 30min immediately after darkening.

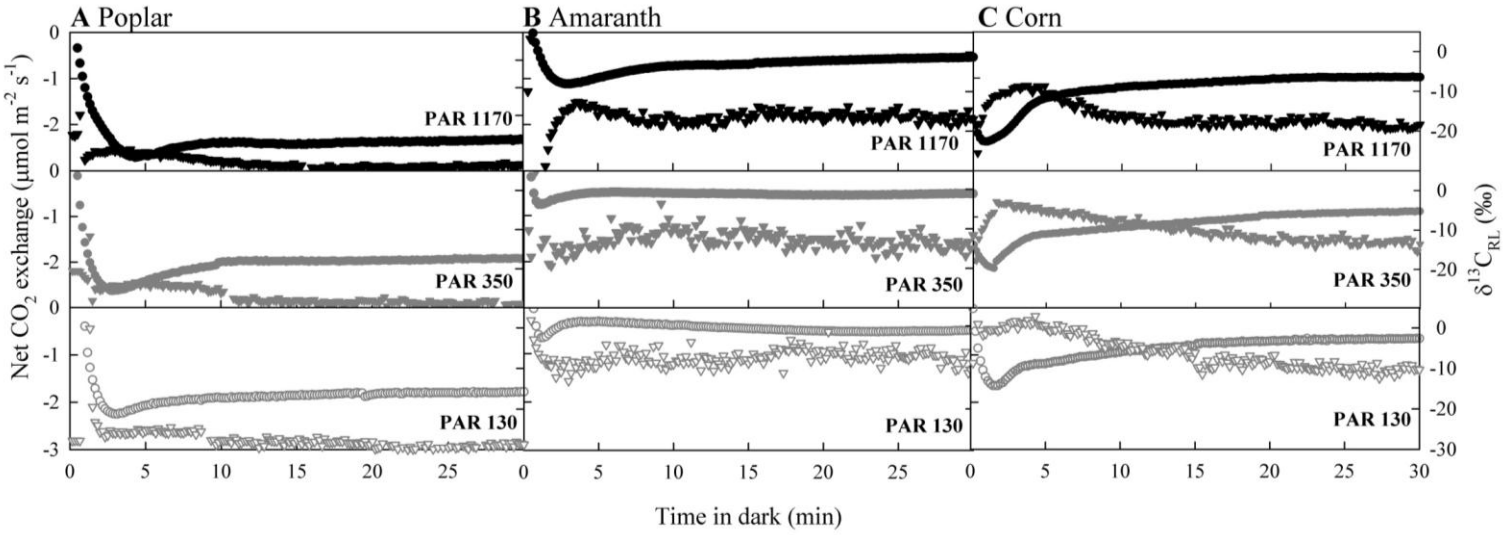

Figure 4. Isotopic signature of LEDR. Average $\delta^{13}C_{RL}$ (black symbols) and average net CO_2 exchange (white symbols) versus photosynthetic rate for *P. deltoides* (**A**), *A. hypochondriacus* (**B**) and *Z. mays* (**C**) at 1170 (squares), 350 (triangles) and130 (circles) PAR. Error bars are standard deviations, n = 9.

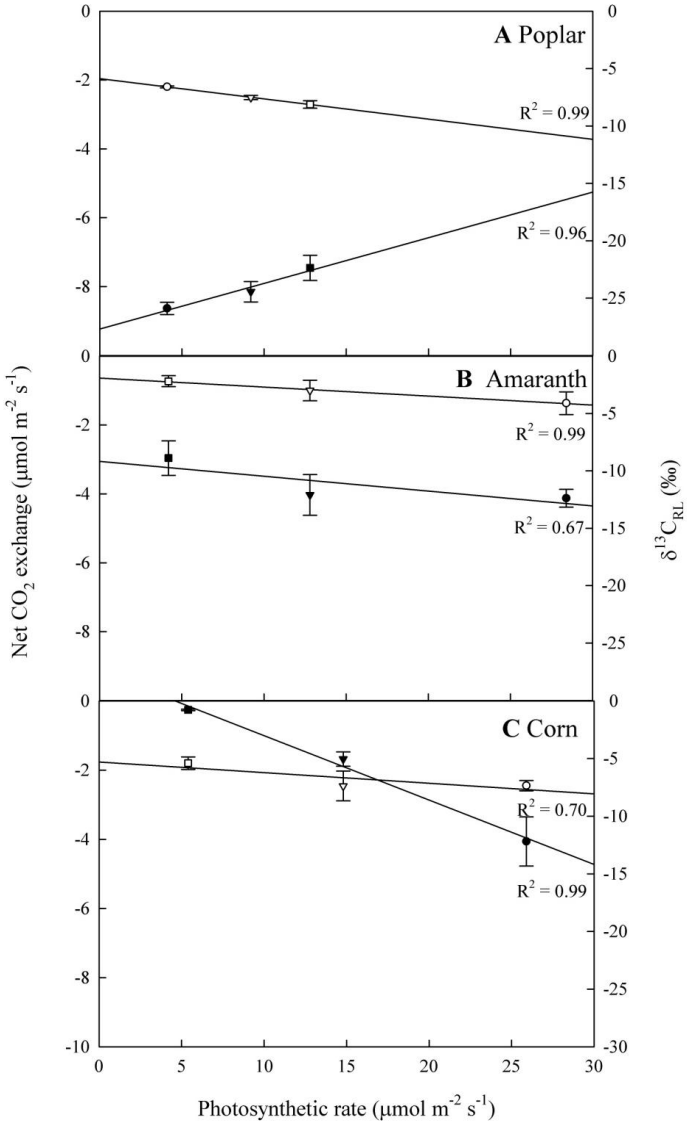

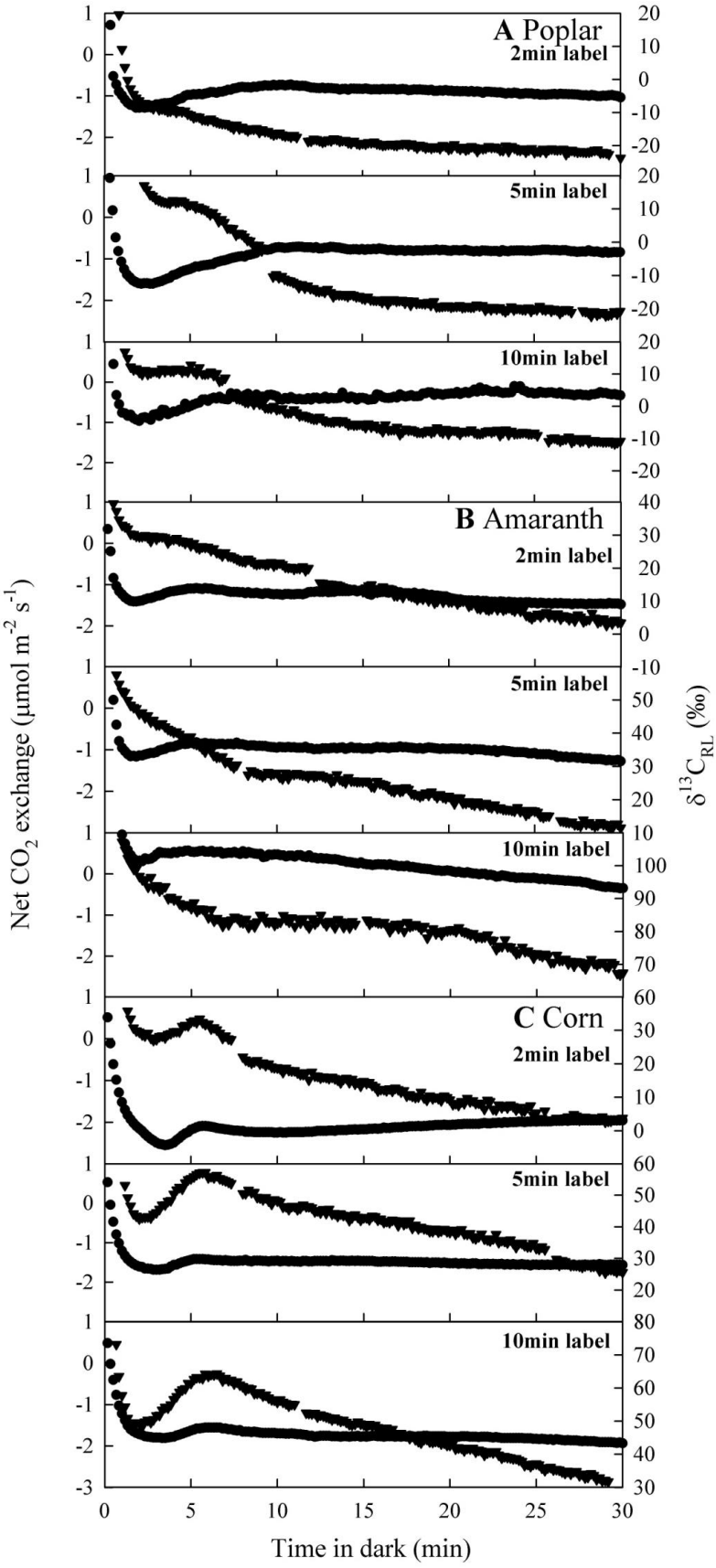

Figure 5. Labeling Experiment. Net CO_2 exchange (circles) and corresponding $\delta^{13}C_{RL}$(triangles) for *P. deltoides* (**A**), *A. hypochondriacus* (**B**) and *Z. mays* (**C**). Enriched $^{13}CO_2$ (+148 ‰) was given for 2, 5 or 10min at 1170 PAR prior to dark period. *Note different right y-axis but same range in every plot.*

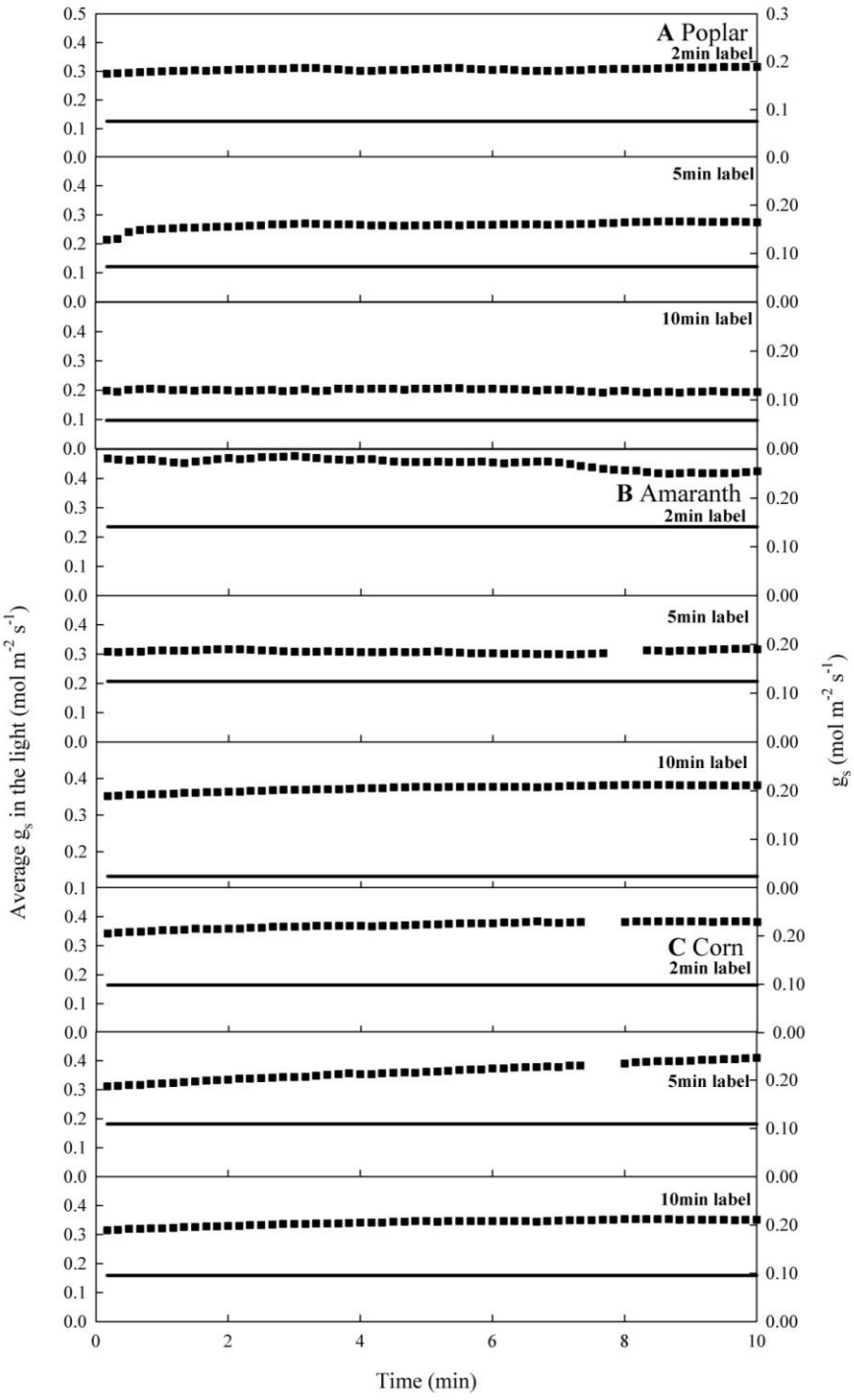

Figure 6. Stomatal conductance. Stomatal conductance (g_s) during LEDR labeling (black squares) and 30sec average before dark acclimation (straight line) for *P. deltoides* (**A**), *A. hypochondriacus* (**B**), and *Z. mays* (**C**).

Figure 7. PEPc activity: PEPc activity of *P. deltoides*, *A. hypochondriacus* and *Z. mays* exposed to 1170 PAR ($p<0.001$). Data shown calculated from 5 leaf samples used in LEDR analysis without label.

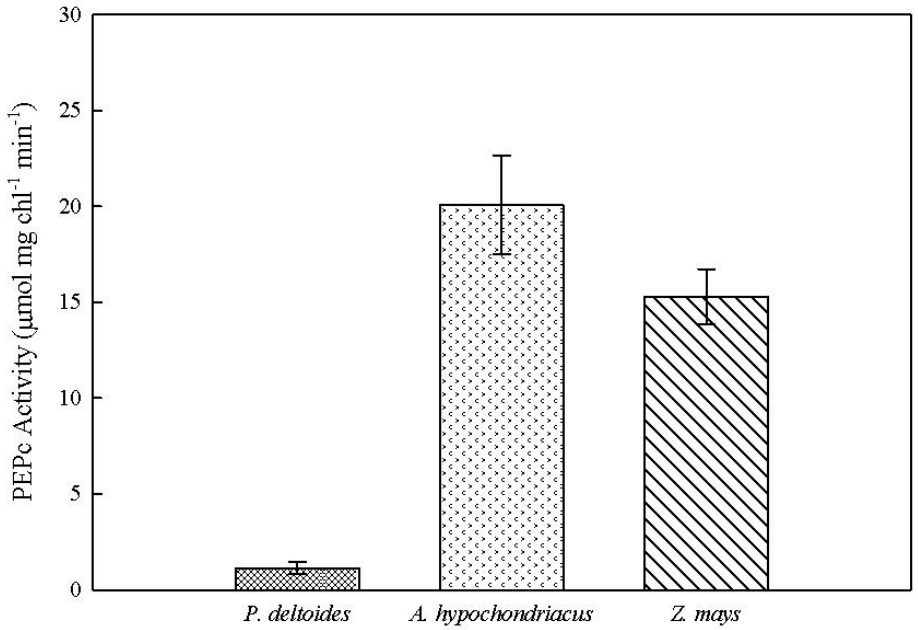

Figure 8. $\delta^{13}C_{RL}$ Label Source. Schematic of LEDR response to Label in *P. deltoides* (C_3), *A. hypochondriacus* (C_4 NAD-ME), and *Z. mays* (C_4 NADP-ME). Potential sources of CO_2 evolution and pools are pictured below each response.

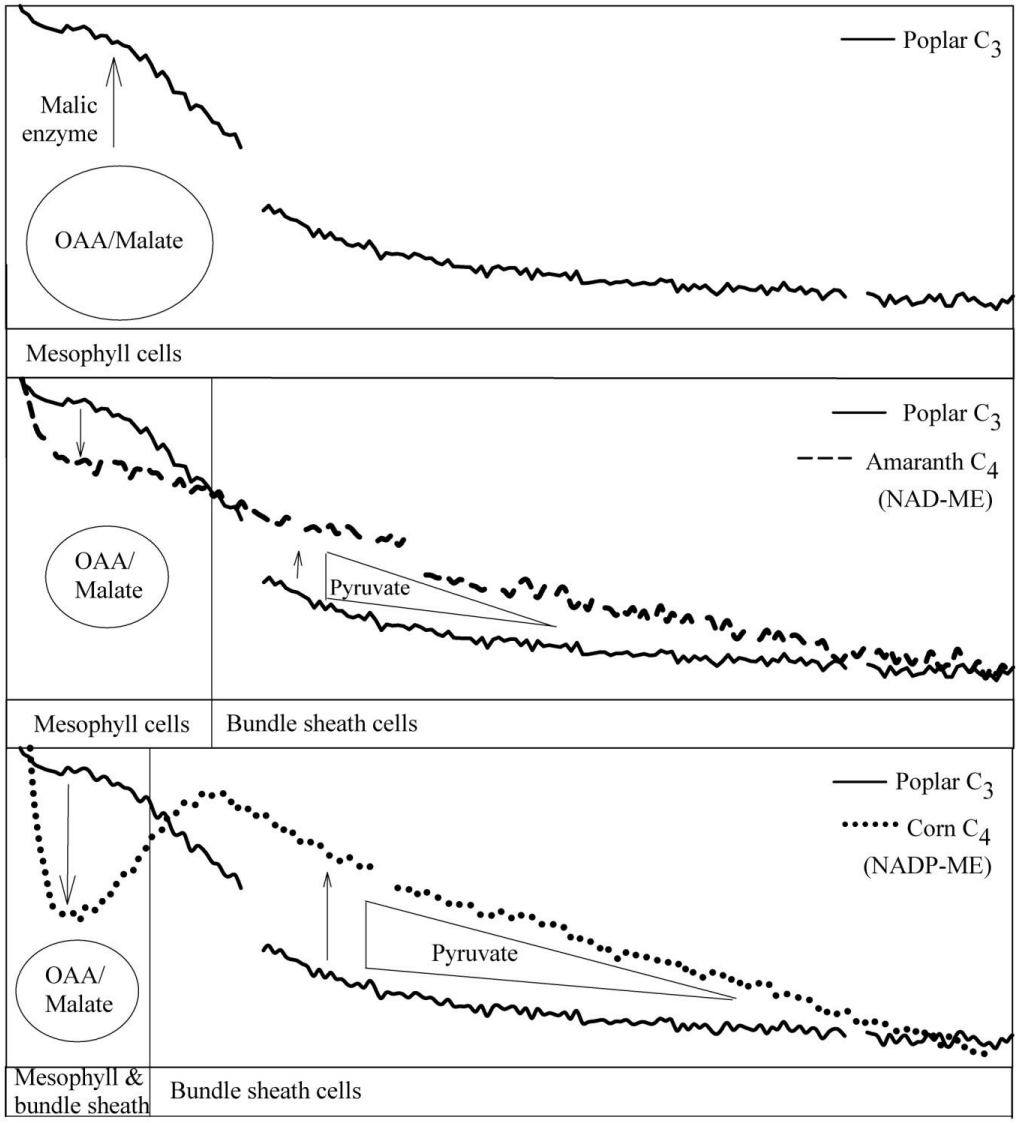

Table 1. **LEDR peak and steady state values.** Values for net CO_2 exchange and $\delta^{13}C_{RL}$ during LEDR and steady state (25min after dark acclimination) for *P. deltoides*, *A. hypochondriacus* and *Z. mays*, n = 4.

Plant Species	Light Intensity (μmol photons m^{-2} s^{-1})	Net CO_2 exchange (μmol m^{-2} s^{-1}) LEDR	Net CO_2 exchange (μmol m^{-2} s^{-1}) Steady state	$\delta^{13}C_{RL}$ (‰) LEDR	$\delta^{13}C_{RL}$ (‰) Steady state
P. deltoides	1172.2 (± 3.0) 351.9 (± 3.5) 131.0 (± 2.6)	-2.71(± 0.03) -2.51 (± 0.06) -2.22 (± 0.11)	-2.06 (± 0.24) -1.95 (± 0.59) -1.80 (± 0.47)	-22.37 (± 0.90) -24.45 (± 1.02) -25.90 (± 0.74)	-28.76 (± 0.38) -28.35 (± 0.17) -29.56 (± 0.19)
A. hypochondriacus	1171.0 (± 2.0) 350.0 (± 3.0) 129.7 (± 1.7)	-1.37 (± 0.33) -1.00 (± 0.30) -0.73 (± 0.16)	-0.84 (± 0.34) -0.69 (± 0.23) -1.90 (± 0.19)	-12.39 (± 0.78) -12.10 (± 1.77) -8.89 (± 1.50)	-15.85 (± 0.45) -12.63 (± 0.80) -8.79 (± 1.36)
Z. mays	1172.0 (± 2.0) 351.9 (± 4.0) 131.5 (± 0.9)	-2.45 (± 0.15) -2.46 (± 0.43) -1.80 (± 0.18)	-1.91 (± 0.09) -1.12 (± 0.30) -0.74 (± 0.11)	-12.19 (± 2.13) -5.04 (± 0.62) -0.78 (± 0.06)	-17.45 (± 0.36) -14.39 (± 2.30) -9.54 (± 0.27)

Table 2. **Photosynthetic values in the Light.** Values for photosynthetic rate (A), stomatal conductance (g_s), internal CO_2 concentration (C_i), and discrimination (Δ) recorded under each light intensity prior to dark period for *P. deltoides*, *A. hypochondriacus* and *Z. mays*, n = 6. All leaves were provided 400 μmol CO_2 mol^{-1} at a flow rate of 600μmol s^{-1}.

Plant Species	Light Intensity (μmol photons m^{-2} s^{-1})	Photosynthetic rate A (μmol m^{-2} s^{-1})	Stomatal conductance g_s (mol m^{-2} s^{-1})	Discrimination Δ (‰)
C_3: *P. deltoides*	1172.2 (± 3.0) 351.9 (± 3.5) 131.0 (± 2.6)	12.8 (± 0.3) 9.2 (± 0.2) 4.1 (± 0.1)	0.2 (± 0.02) 0.2 (± 0.01) 0.1 (± 0.003)	19.3 (± 0.5) 21.8 (± 0.9) 26.7 (± 0.04)
C_4 NAD-ME: *A. hypochondriacus*	1171.0 (± 2.0) 350.0 (± 3.0) 129.7 (± 1.7)	28.4 (± 2.0) 12.8 (± 0.6) 4.2 (± 0.5)	0.4 (± 0.09) 0.3 (± 0.03) 0.07 (± 0.02)	4.5 (± 0.4) 3.9 (± 0.2) 1.6 (± 0.2)
C_4 NADP-ME: *Z. mays*	1172.0 (± 2.0) 351.9 (± 4.0) 131.5 (± 0.9)	25.9 (± 1.2) 14.8 (± 1.9) 5.4 (± 0.8)	0.8 (± 0.3) 0.2 (± 0.1) 0.07 (± 0.02)	4.8 (± 0.6) 4.0 (± 0.6) 4.1 (± 0.5)

Table 3. **2, 30 and 70min labeled LEDR dynamics.** Values for net CO_2 exchange and $\delta^{13}C_{RL}$ at 2, 30 and 70min after dark acclimation and application of $^{13}CO_2$ label, n = 4. P-values correspond to one-way ANOVAS.

Plant Species	$^{13}CO_2$ Labeling time (min)	Net CO_2 exchange ($\mu mol\ m^{-2}\ s^{-1}$) 2min	Net CO_2 exchange ($\mu mol\ m^{-2}\ s^{-1}$) 30min	Net CO_2 exchange ($\mu mol\ m^{-2}\ s^{-1}$) 70min	$\delta^{13}C_{RL}$ (‰) 2min	$\delta^{13}C_{RL}$ (‰) 30min	$\delta^{13}C_{RL}$ (‰) 70min
P. deltoides	2 5 10	-1.29 (± 0.1) -1.59 (± 0.7) -0.69 (± 0.1) p = 0.04	-1.01 (±0.5) -0.84 (± 0.4) -0.25 (±0.1) p = 0.04	-1.08 (± 0.1) -0.92 (± 0.2) -0.33 (± 0.1) p = 0.00	-7.42 (± 3.9) 11.05 (± 2.8) 11.61 (± 1.0) p = 0.00	-23.83 (± 2.5) -22.17 (± 3.4) -10.84 (± 5.6) p = 0.03	-24.32 (± 1.5) -22.67 (± 1.0) -12.62 (± 0.9) p = 0.00
A. hypochondriacus	2 5 10	-1.22 (± 0.2) -2.13 (± 0.1) 0.35 (± 0.6) p = 0.00	-1.56 (± 0.2) -1.16 (± 0.1) -0.17 (± 0.1) p = 0.00	-1.36 (± 0.1) -1.40 (± 0.9) -0.37 (± 0.1) p = 0.05	29.25 (± 6.8) 39.89 (± 14.15) 98.16 (± 21.2) p = 0.01	6.90 (± 4.3) 13.51 (± 7.2) 70.81 (± 5.7) p = 0.00	0.83 (± 0.1) 7.87 (± 6.3) 64.89 (± 9.2) p = 0.00
Z. mays	2 5 10	-2.24 (± 0.4) -1.72 (± 0.1) -1.80 (± 0.2) p = 0.05	-1.62 (± 0.3) -1.55 (± 0.1) -1.92 (± 0.1) p = 0.06	-1.86 (± 0.2) -1.75 (± 0.1) -2.12 (± 0.1) p = 0.01	LEDR peak: 27.02 (± 5.3); 42.55 (± 3.9); 49.20 (± 9.2); p=0.01 Post-LEDR: 33.37 (± 12.8); 57.03 (± 9.4); 64.21 (± 13.6); p=0.02	9. 25 (± 6.7) 25.33 (± 8.2) 25.01 (± 7.1) p = 0.02	0.61 (± 1.9) 17.17 (± 5.8) 16.31 (± 4.0) p = 0.01